



Dipetidyl peptidase-4 and transferrin receptor serve as prognostic biomarkers for acute myeloid leukemia

Jie Wei^{1#}, Guan Ye Nai^{2#}, Yi Dai^{3#}, Xun Jun Huang¹, Ming Yue Xiong¹, Xiang You Yao¹, Zhi Ning Huang¹, Si Nian Li¹, Wei Jie Zhou⁴, Yan Huang¹, Peng Cheng³, Dong Hong Deng³

¹Department of Hematology, Baise People's Hospital, Baise, China; ²Department of hematology, The Affiliated Hospital of Youjiang Medical University for Nationalities, Baise, China; ³Department of Hematology, The First Affiliated Hospital of Guangxi Medical University, Nanning, China; ⁴Department of Clinical Laboratory, Baise People's Hospital, Baise, China

Contributions: (I) Conception and design: J Wei, GY Nai, Y Dai; (II) Administrative support: XJ Huang, MY Xiong; (III) Provision of study materials or patients: DH Deng, P Cheng; (IV) Collection and assembly of data: ZN Huang, SN Li; (V) Data analysis and interpretation: Y Huang, WJ Zhou; (VI) Manuscript writing: All authors; (VII) Final approval of manuscript: All authors.

[#]These authors contributed equally to this work.

Correspondence to: Yan Huang. Department of Hematology, Baise People's Hospital, Baise, China. Email: hygn2000@163.com; Peng Cheng. Department of Hematology, The First Affiliated Hospital of Guangxi Medical University, Nanning 530000, China. Email: gxchengpeng@163.com; Dong Hong Deng. Department of Hematology, The First Affiliated Hospital of Guangxi Medical University, Nanning, China. Email: ddh_gx@163.com.

Background: Acute myeloid leukemia (AML) is the most common hematological malignancy in adult patients. Ferroptosis-related signatures have been shown to act as regulators of the progression of multiple cancer types, but the role of ferroptosis in AML remains to be elucidated. We performed the present study to preliminarily investigate the roles of ferroptosis-related genes (FRGs) in AML.

Methods: The transcriptome data of AML patients was downloaded from The Cancer Genome Atlas (TCGA) and the transcriptome data of normal samples was obtained from the Genotype-Tissue Expression (GTEx) database. FRGs were selected via public articles. Expression levels of FRGs between AML and normal samples were analyzed. The prognostic model based on FRGs was constructed via lasso regression. The expression levels and prognostic role of FRGs were identified from the risk model. We also performed validation experiments to verify the expression levels of the final selected genes via immunohistochemistry, polymerase chain reaction (PCR), and RNA-seq. Finally, we explored the associations between immune infiltration, drug sensitivity, and the selected FRGs.

Results: The transcriptome data of 151 AML samples were retrieved from TCGA and 70 bone marrow normal samples were retrieved from the GTEx database. Additionally, 23 FRGs were collected from the published articles. There were 22 differentially expressed FRGs, and among them, dipetidyl peptidase-4 (DPP4) ($P=0.011$, HR =1.504), GPX4 ($P=0.055$, HR =1.569), LPCAT3 ($P<0.001$, HR =2.243), SLC7A11 ($P=0.012$, HR =2.243), and transferrin receptor (TFRC) ($P=0.029$, 0.774) had a significant influence on the prognosis of AML patients via lasso regression. The area under the curve (AUC) values of the 1-, 3-, and 5-year receiver operating characteristic (ROC) curves of the FRG signatures indicated that this model is novel and effective method for predicting the prognosis of AML patients. DPP4 ($P<0.001$) was overexpressed while LPCAT3 ($P<0.001$), TFRC ($P<0.001$), GPX4 ($P<0.001$), and SLC7A11 ($P<0.001$) were downregulated, further validation experiment results indicated that DPP4 was significantly downregulated but TFRC was upregulated in AML samples. Dysregulation of DPP4 and TFRC influence numbers of chemotherapy regimens sensitivity.

Conclusions: DPP4 and TFRC act as biomarkers for predicting and diagnosing AML, and their expression levels also have significant correlations with drug resistance in AML.

Keywords: Acute myeloid leukemia (AML); DPP4; TFRC; prognostics biomarker

Submitted Jun 14, 2021. Accepted for publication Jul 29, 2021.

doi: 10.21037/atm-21-3368

View this article at: <https://dx.doi.org/10.21037/atm-21-3368>

1 Introduction

2 Acute myeloid leukemia (AML) is characterized by a
3 loss of control of myeloid precursor cell proliferation
4 and undifferentiation (1). If AML patients do not
5 undergo appropriate treatment, death can rapidly occur.
6 Anthracycline and cytarabine have remained the standard
7 therapy regimens for AML patients since the 1970s (2).
8 Despite advances in diagnostic and therapeutic methods, the
9 overall survival (OS) of AML patients has not significantly
10 improved. Over the past decade, with the introduction
11 of targeted therapy agents combined with traditional
12 chemotherapy, the rates of complete remission (CR) have
13 been improved, but the rate of relapse is still unchanged.
14 Relapse of disease remains an obstacle for lengthening
15 the OS of AML patients. For high-risk patients, the rate
16 of disease relapse is more than 60% and results in a short
17 median disease-free survival (DFS) of less than 1 year (range,
18 4 to 11 months) (3). To date, several driver mutations
19 have been observed in AML patients, and these mutations
20 have deep influence on the prognosis of AML patients.
21 Kishtagari *et al.* study summarizes the driver mutations
22 in AML, based on the functions of driver genes, they are
23 divided into signal transduction (FLT3, NRAS, KRAS,
24 and KIT), splicing mutations (SF3B1, ZRSR2, U2AF1,
25 and SRSF2), tumor suppressors (TP53, WT1, and TET2),
26 AML licensing mutations (NMP1), epigenetic modifiers
27 (IDH1, IDH2, TET2, SRSF2, BCOR, BCORL, TET2,
28 ASXL1, and EH22), transcription factors (RUNX1,
29 CEBPA, and GATA2), and chromatin modifiers (Cohesin,
30 ASXL1, and EH22) (4). Patients with the mutated NMP1,
31 RUNX1, and TP53 lead to poor prognosis, but biallelic
32 mutated CEBPA indicate favorable prognosis (5). Several
33 studies have also demonstrated the occurrence of targeted
34 therapy resistance (6,7). The target regimens enasidenib
35 and ivosidenib have been used to treat IDH mutated AML
36 patients (8). Sorafenib was used to therapy the with FLT3-
37 ITD mutated AML patients (9). However, the resistance of
38 these target therapy has been found (6,10). These indicated
39 that some unique mutation can be sever as the diagnostic
40 and prognostic biomarkers for AML patients, as well as
41 assessing the drug resistance, relapse risk, and therapy
42 targets markers. Drug resistance and disease relapse may
43 be the main reasons leading to the poor outcomes of AML
44 patients, but the underlying mechanisms are still unclear.
45 It is therefore important to find novel biomarkers for
46 diagnosis, assessing prognosis, monitoring drug resistance,
47 and even supplementary therapy methods for AML patients.
48

Iron is a fundamental inorganic nutrient which has a
critical role in multiple biological processes such as DNA and
RNA synthesis, cellular respiration, immune responses, and
detoxification processes, among others (11). Ferroptosis was
introduced in 2012 and is defined as a unique iron-dependent
form of cell death. The features of ferroptosis include
smaller mitochondria with increased membrane density,
and decreased mitochondrial cristae (12). Ferroptosis strike
the death balance in common cells and tissues (13). Several
studies have demonstrated that ferroptosis is a significant
regulator of tumor progression (14-16). Ferroptosis is
regulated via several factors, and ferroptosis-related genes
(FRGs) may be the most significant regulators among them.
FRGs have been observed to be differentially expressed and
play key roles in the prognosis of various cancer types such
as pancreatic cancer, glioma, and hepatocellular carcinoma
(17-20). From these findings, it is clear that FRGs have
been well investigated in solid tumors. In regards to AML,
several studies have explored the mechanism of drug-
induced ferroptosis (21-23). Du *et al.*'s study indicated that
DHA can inhibit leukemia cell proliferation via inducing
ferroptosis (21). Furthermore, Du *et al.* revealed that
inhibition of ferroptosis can promote ATPR-induced AML
cell differentiation by regulating the ROS-autophagy-
lysosomal pathway (22). Zhu *et al.* showed that typhaneoside
inhibited leukemia cell proliferation via inducing ferroptosis-
related autophagy (23). These findings indicate that inducing
ferroptosis may be a novel potential anticancer method
for AML. However, there have been no studies that have
investigated FRG expression levels, their prognostic role, and
their association with the tumor microenvironment (TME)
and drug resistance in AML patients. In the present study,
we used bioinformatics to analyze FRG expression levels,
their prognostic role, and their association with immune
infiltration and drug sensitivity. Furthermore, we collected
normal samples and AML patient samples to validate the
gene expression levels via immunohistochemistry, polymerase
chain reaction (PCR), and next-generation sequencing
(NGS). We present the following article in accordance
with the REMARK reporting checklist (<https://dx.doi.org/10.21037/atm-21-3368>).

Methods

Raw data

The transcriptome data and clinical data of 151 AML
samples from The Cancer Genome Atlas (TCGA) database

97 and 70 bone marrow normal samples from the Genotype-
 98 Tissue Expression (GTEx) database were collected from
 99 the University of California Santa Cruz database (UCSC
 100 Xena, <https://xenabrowser.net/datapages/>). Subsequently,
 101 log₂ (FPKM+1) normalization was performed on the
 102 transcriptome data. We searched and extracted 23 FRGs
 103 from PubMed (24-26).

104

105

106

Screening differentially expressed FRGs

107 We screened differentially expressed FRGs between the
 108 TCGA-LAML cohort (tumor) and the GTEx cohort
 109 (normal) for further analysis. Differential analysis was
 110 carried out with the Wilcoxon test in R software. A heatmap
 111 plot of differentially expressed genes was generated via
 112 the ggplot2 package. P<0.05 was considered statistically
 113 significant.

114

115

116

Construction of the ferroptosis-related prognostic signature

117 We obtained prognostic FRGs via univariate cox regression
 118 based on differential expression of FRGs, then used
 119 lasso regression to obtain a more refined signature by
 120 constructing a penalty function. Multivariate cox regression
 121 (stepwise) was used to construct the final prognostic
 122 signature. KM survival analysis was used to generate
 123 the survival curves based on median values, and log-
 124 rank P<0.05 was considered statistically significant. The
 125 receiver operating characteristic (ROC) curves, nomogram,
 126 and calibration curve of the prognostic signature were
 127 generated via the R packages survivalROC, survminer, and
 128 rms, respectively. P<0.05 was considered as statistically
 129 significant.

130

131

132

Tumor immune infiltration analysis

133 We used the CIBERSORT algorithm of tumor immune cell
 134 infiltration to calculate the abundance of 22 immune cells
 135 in the TCGA-LAML cohort. The correlation analysis of
 136 immune cells was carried out via the Spearman method.

137

138

139

Immunohistochemistry

140 Bone marrow smears of AML and normal cases were
 141 collected, fixed with 10% neutral formalin, dehydrated
 142 with gradient alcohol, and stained with hematoxylin
 143 and eosin (HE). The following antibodies were used for
 144 immunostaining: dipetidyl peptidase-4 (DPP4) (Abcam,

ab187048), GPX4 (Proteintech, 14432-1-AP), LPCAT3
 (Abcam, ab239585), SLC7A11 (Proteintech, 26864-1-
 AP), and transferrin receptor (TFRC) (Proteintech,
 10084-2-AP).

145

146

147

148

149

150

151

152

153

154

155

156

157

158

159

160

161

162

163

164

165

166

167

168

169

170

171

172

173

174

175

176

177

178

179

180

181

182

183

184

185

186

187

188

189

190

191

192

PCR

EDTA anticoagulant tubes were used to collect the
 peripheral blood of healthy adults and AML patients,
 and Trizol (Invitrogen, China) was used to extract total
 RNA. Then, the concentration of total RNA was detected
 by a nucleic acid analyzer. GeneRuler DNA Ladder Mix
 and Maxima Reverse Transcriptase were used to reverse
 transcribe RNA into cDNA, and gene expression levels
 were detected according to the 2X SG Fast qPCR Master
 Mix (High Rox, B639273, BBI, ABI) kit instructions.
 GAPDH was used as an internal reference, and the results
 were calculated using the 2^{-ΔΔCt} method.

RNA-sequence (RNA-seq)

EDTA anticoagulant tubes were used to collect the
 peripheral blood of healthy adults and AML patients, and
 Trizol (Invitrogen, China) was used to extract total RNA.
 RNA samples were used to perform NGS. The library
 construction and transcriptome sequencing were completed
 by Sheng Gong Bioengineering (Shanghai) Co., Ltd.

Drug sensitivity analysis based on risk score

The R package pRRophetic was used to perform the drug
 sensitivity analysis.

Statistical analysis

The differential FRGs were screened through the Wilcoxon
 method. Kaplan-Meier (KM) plots were used to analyze the
 differential survival between groups, and log-rank P<0.05
 was considered statistically significant. Univariate cox
 regression, lasso regression, and multivariate (stepwise) cox
 regression were used to construct the prognostic signature.
 Wilcoxon and Spearman tests were used for difference
 analysis and correlation analysis, respectively. P<0.05 was
 considered statistically significant.

Ethical statement

The study was conducted in accordance with the

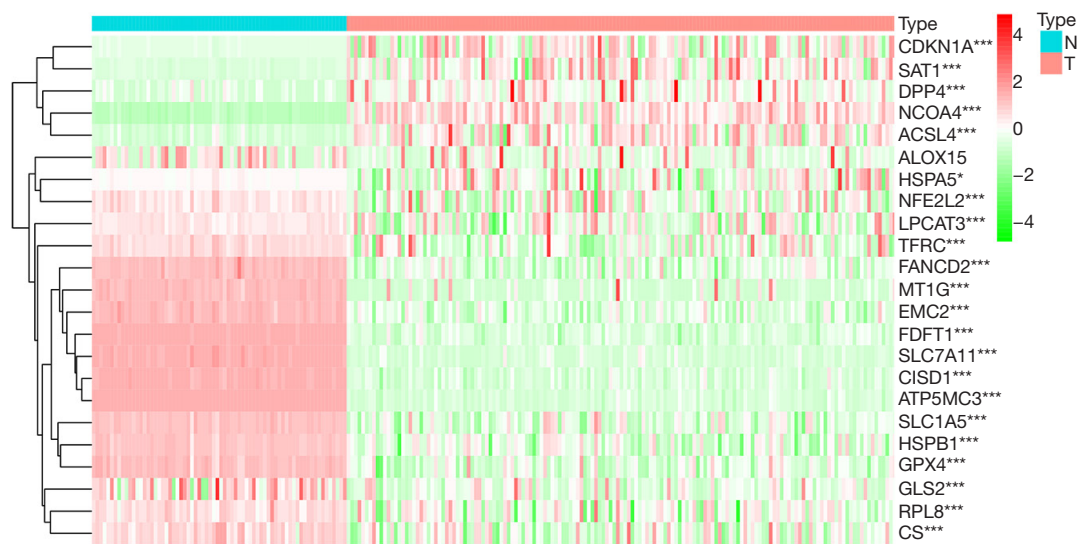


Figure 1 Differential expression of ferroptosis-related genes in acute myeloid leukemia patients. Red represents genes with high expression, and green represents genes with low expression. *, *** represent $P < 0.05$, and $P < 0.001$, respectively.

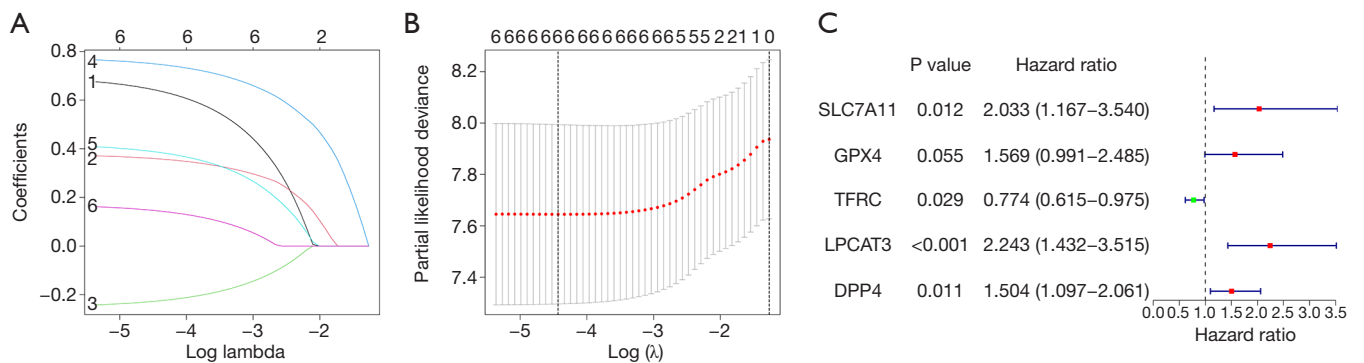


Figure 2 Construction of the FRG prognostic signature for acute myeloid leukemia. (A,B) Selection of the optimal λ threshold for lasso regression. (C) The forest graph of the FRG prognostic signature. FRG, ferroptosis-related gene.

193 Declaration of Helsinki (as revised in 2013).

194

195 **Results**

196 *Differential expression of FRGs in AML patients*

197 We retrieved 23 FRGs from PubMed and analyzed the
 198 differential expression of FRGs between AML (n=151)
 199 and normal bone marrow (n=70). The heatmap plot
 200 showed that there were 22 differentially expressed FRGs
 201 (Figure 1).
 202
 203

Establishment of the FRG prognostic signature for AML

204 We obtained 7 FRGs that affected the OS of AML patients
 205 via univariate cox regression of differentially expressed
 206 FRGs. The results of lasso regression indicated that $\lambda = -4.4$
 207 was the optimal value, then 6 FRGs were obtained for
 208 further analysis (Figure 2A,2B). Finally, a 5-FRG prognostic
 209 signature was established for AML (Figure 2C).
 210

211 A heatmap was generated showing the FRG signature's
 212 gene expression in low-risk and high-risk samples
 213 (Figure 3A). The risk score curve and survival status plot
 214

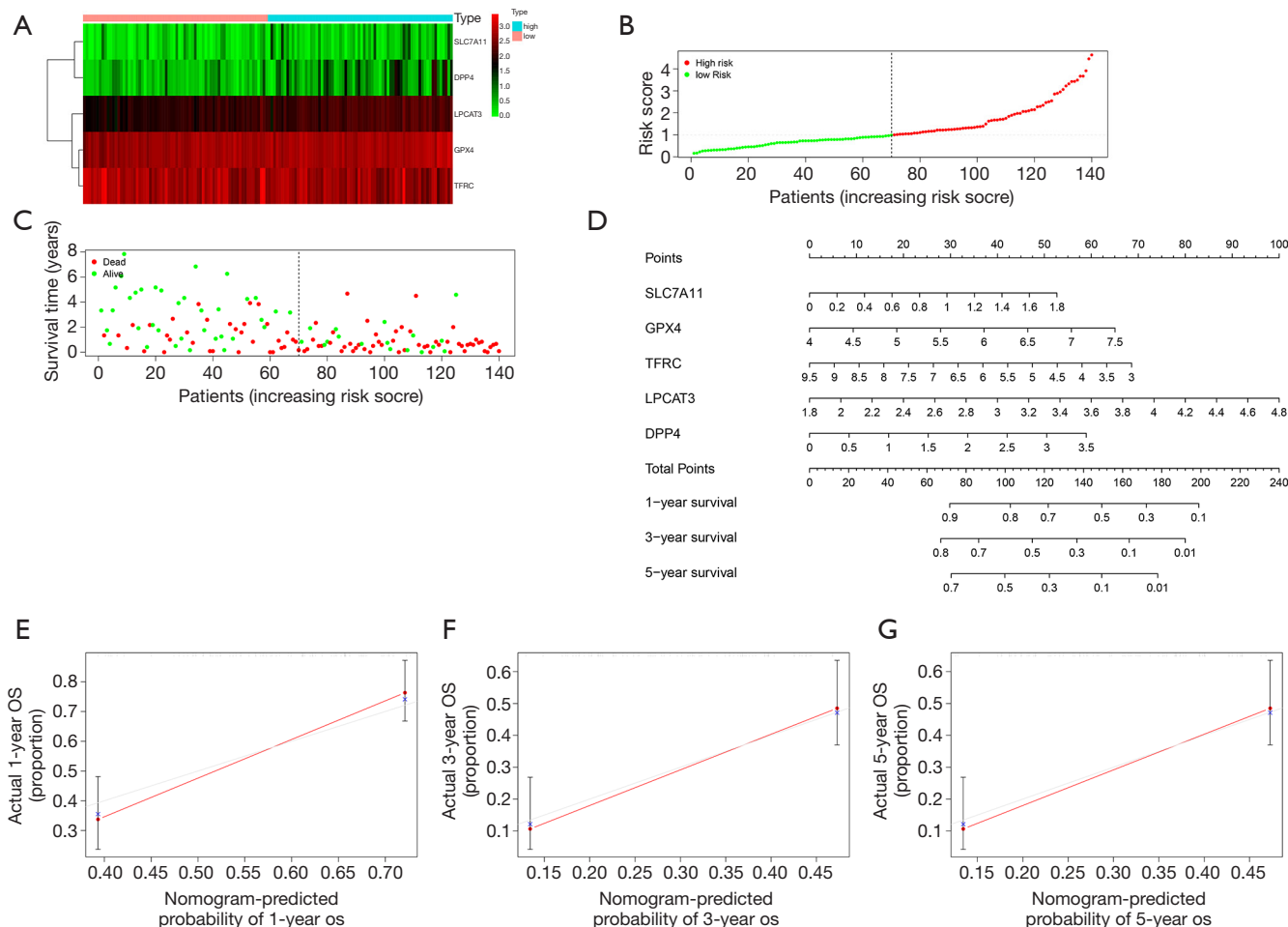


Figure 3 The expression of the signature genes, risk score curve, survival status, nomogram, and calibration curve of the FRG prognostic signature. (A) Heatmap of the expression of FRG signature genes in low- and high-risk samples. Red represents high expression and green represents low expression. (B) Risk score curve of the FRG prognostic signature. Dotted lines represent the boundaries between high- and low-risk groupings. (C) Survival status plot of the FRG prognostic signature. (D) Nomogram of the FRG prognostic signature. The 1-year (E), 3-year (F), and 5-year (G) calibration curves of the nomogram. X-axis and Y-axis represent the predicted survival and actual survival probability of patients' overall survival, respectively. FRG, ferroptosis-related gene. FRG, ferroptosis-related gene.

215 indicated that low and high-risk could well distinguish
 216 between surviving and dead patients (Figure 3B,3C). The
 217 nomogram and calibration curves demonstrated that the
 218 FRG prognostic signature had perfect predictive ability
 219 (Figure 3D-3G).

220 **KM survival analysis and ROC curve of the FRG signature**

221
 222
 223 The area under curve (AUC) values of the 1-, 3-, and 5-year
 224 ROC curves of the FRG signature were 0.804, 0.785,
 225 and 0.930, respectively (Figure 4A). KM survival analysis
 226

227 indicated that patients with low risk had a better OS for
 228 AML (log-rank $P < 0.001$) (Figure 4B).

229 **FRG expression levels and their association with prognosis**

230
 231
 232 There were 5 genes in the FRG signature, namely *DPP4*,
 233 *LPCAT3*, *TFRC*, *GPX4*, and *SLC7A11*. *DPP4* was highly
 234 expressed in tumors compared with normal samples
 235 (Figure 5A), while *LPCAT3*, *TFRC*, *GPX4*, and *SLC7A11*
 236 were lowly expressed in tumor samples (Figure 5B-5E). In
 237 terms of prognosis, high expression of *DPP4*, *LPCAT3*,
 238

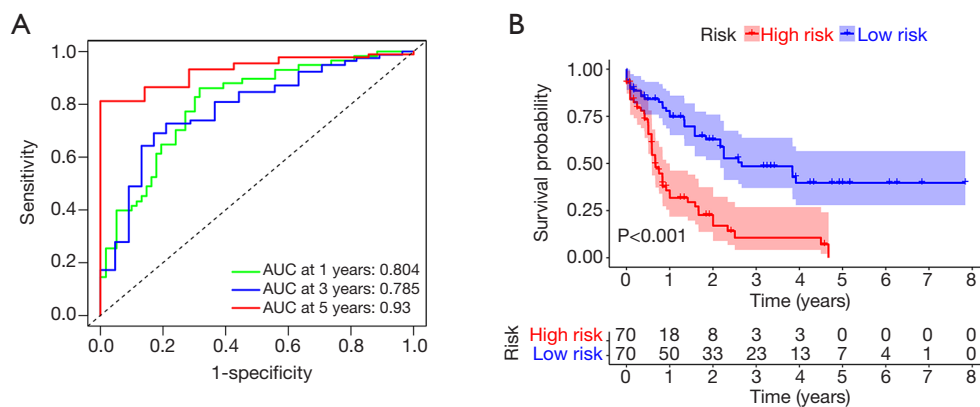


Figure 4 KM survival analysis and ROC curve of the FRG signature. (A) The ROC curves of the FRG signature. Green, blue, and red represent 1-year, 3-year, and 5-year ROC curves, respectively. (B) KM survival analysis of high and low risk of FRG signature. KM, Kaplan-Meier; ROC, receiver operating characteristic; AUC, area under curve; FRG, ferroptosis-related gene.

239 *GPX4*, and *SLC7A11* resulted in a shorter OS, while high
240 expression of TFRC resulted in a better OS in AML
241 patients (Figure 5F-5J).

242 243 *The relative abundance and correlation of 22 immune cells* 244 *in the TCGA-LAML cohort* 245

246 The histogram shows the relative abundance of 22 immune
247 cells in the TCGA-LAML cohort (Figure 6A). The heatmap
248 of correlations between the 22 immune cells indicated
249 that M2 macrophages were negatively correlated with
250 other immune cells, and resting mast cells were positively
251 correlated with other immune cells (Figure 6B).

252 253 *Prognostic immune cells in AML patients* 254

255 KM survival analysis indicated that high infiltration
256 of resting mast cells resulted in a better OS in AML
257 patients (Figure 7A). Nevertheless, high infiltration of M2
258 macrophages resulted in a poor prognosis (Figure 7B).

259 260 *Correlation between the FRG signature biomarker and the* 261 *abundance of resting mast cells and M2 macrophages* 262

263 Spearman correlation analysis demonstrated that DPP4
264 was negatively correlated with resting mast cells and M2
265 macrophages (Figure 8A). GPX4 was positively correlated
266 with resting mast cells but negatively correlated with
267 M2 macrophages (Figure 8B). LPCAT3 was positively
268 correlated with resting mast cells but negatively correlated
269

270 with M2 macrophages (Figure 8C). *SLC7A11* was positively
271 correlated with resting mast cells but negatively correlated
272 with M2 macrophages (Figure 8D). TFRC was negatively
273 correlated with resting mast cells but positively correlated
274 with M2 macrophages (Figure 8E).

275 276 *The results of validation experiments* 277

278 The results of immunohistochemistry indicated that
279 DPP4, GPX4, LPCAT3, *SLC7A11*, and TFRC had higher
280 expression in AML bone marrow samples (Figure 9).
281 Furthermore, PCR results showed that TFRC ($P < 0.01$)
282 was significantly overexpressed, but DPP4 ($P < 0.01$), GPX4
283 ($P < 0.01$), LPCAT3 ($P < 0.01$), and *SLC7A11* ($P < 0.01$)
284 were significantly downregulated in AML samples (Figure 10). To
285 further validate these selected gene expression levels between
286 normal and AML samples, RNA-seq was performed, and the
287 results showed that TFRC was significantly overexpressed
288 in AML samples ($P = 2.13 \times 10^{-6}$), while DPP4 ($P = 0.016$) was
289 significantly downregulated in AML samples (<https://cdn.amegroups.cn/static/public/atm-21-3368-1.xls>).
290

291 292 *Drug sensitivity* 293

294 The ultimate goal of cancer research is finding novel or
295 complementary therapy regimens for cancer patients. We
296 used TFRC and DPP4 to divide AML patients into high-
297 and low-risk score groups, and explored the association
298 between risk score and drug sensitivity. The results showed
299 that patients with downregulation of TFRC were resistant
300

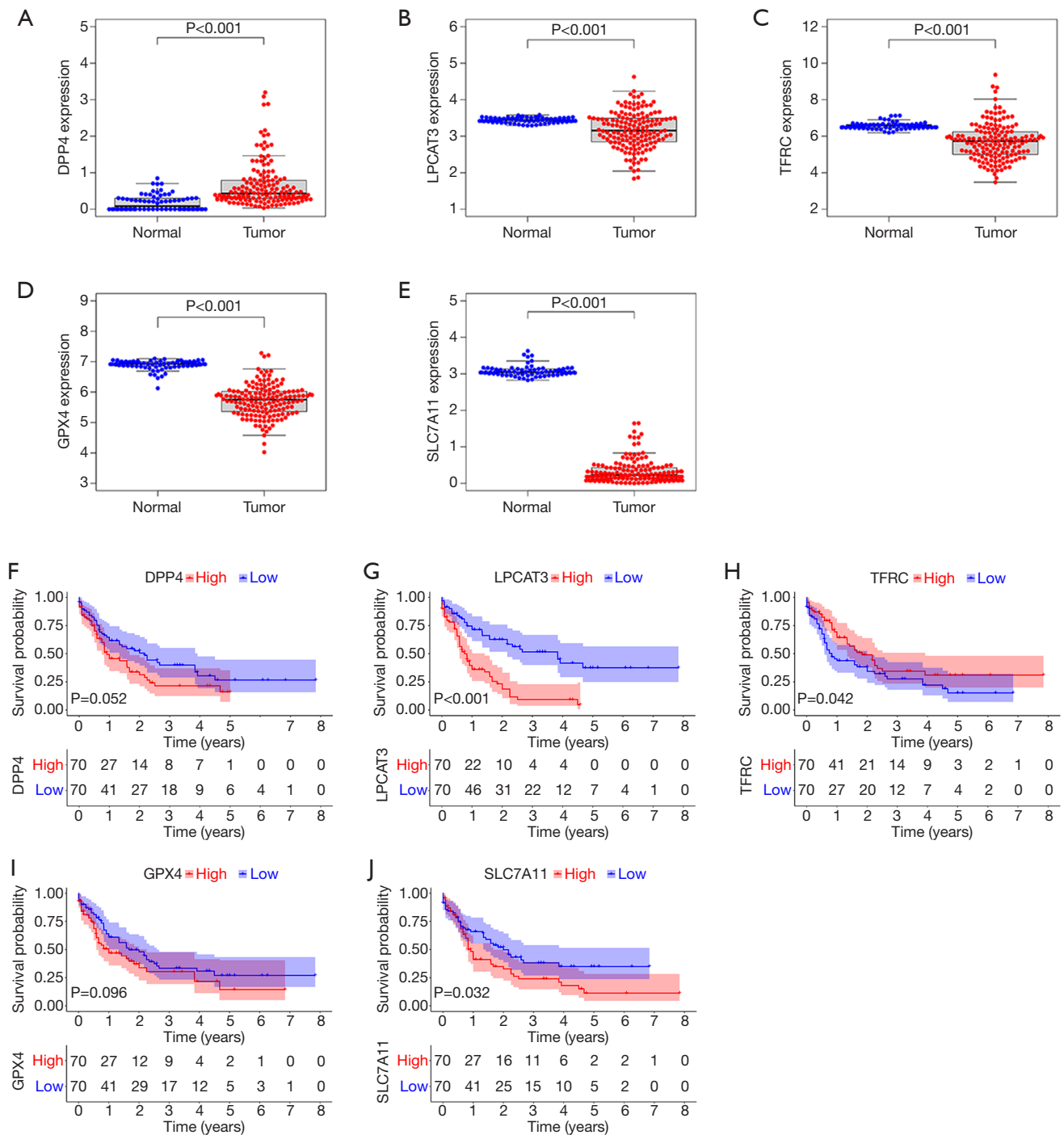


Figure 5 FRG expression levels and their association with prognosis. Expression levels of (A) DPP4, (B) LPCAT3, (C) TFRC, (D) GPX4, and (E) SLC7A11 in tumor and normal samples. Kaplan-Meier survival analysis of expression levels and overall survival based on (F) DPP4, (G) LPCAT3, (H) TFRC, (I) GPX4, and (J) SLC7A11. FRG, ferroptosis-related gene.

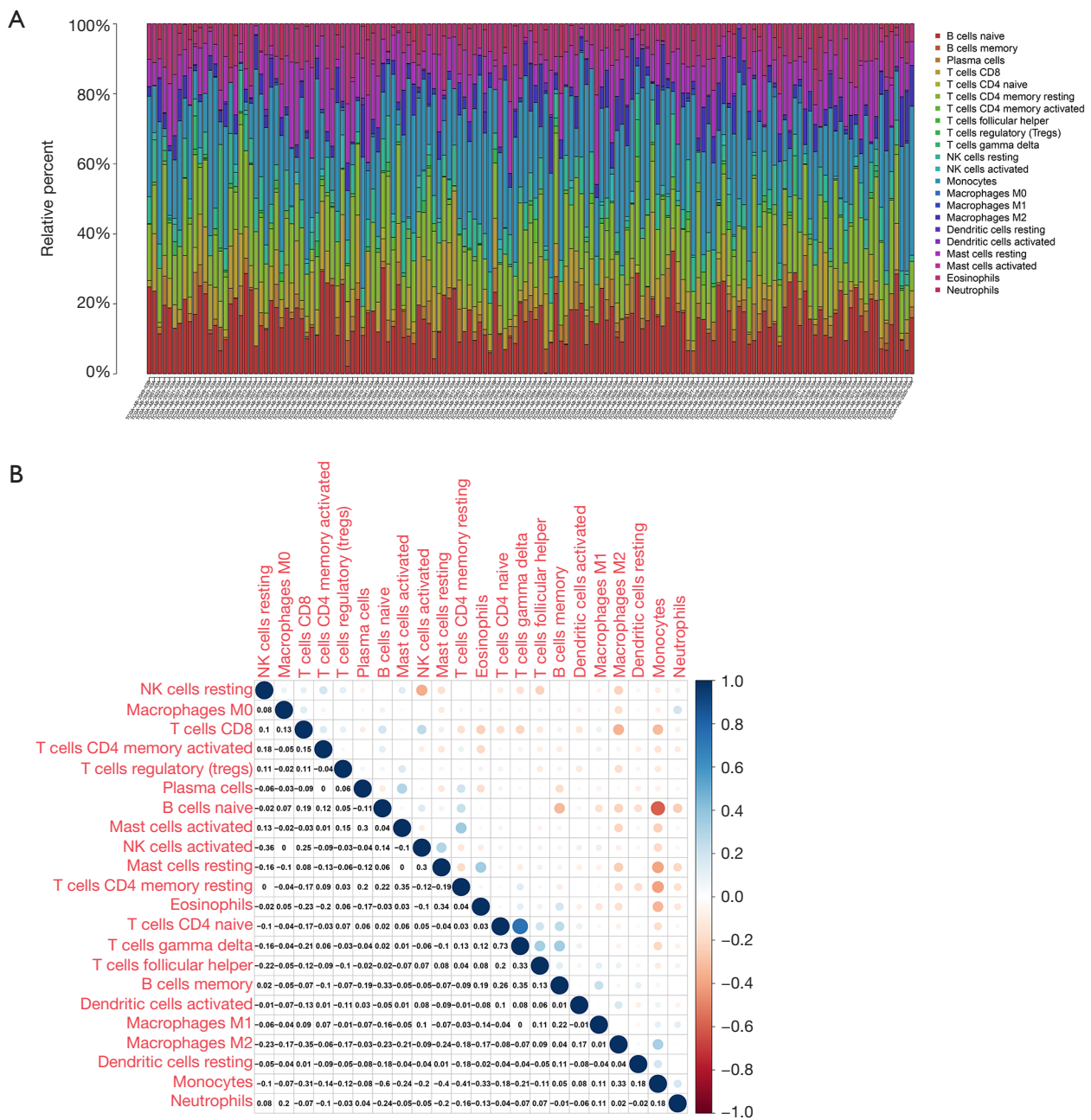


Figure 6 The relative abundance and correlation of 22 immune cells in the TCGA-LAML cohort. (A) Histogram of the relative abundance of 22 immune cells. (B) Heatmap of correlations between the 22 immune cells. Blue and red represent positive and negative correlation, respectively.

to many drugs such as ATRA, axitinib, and vinorelbine, among others, but sensitive to dasatinib, bryostatins, and so on (Figure 11). According to DPP4, the sensitivity analysis revealed that patients with scores based on the DPP4 group were resistant to CMK and cytarabine, and among others,

but sensitive to dasatinib (Figure 12).

Discussion

With the better learning the critical role of ferroptosis in

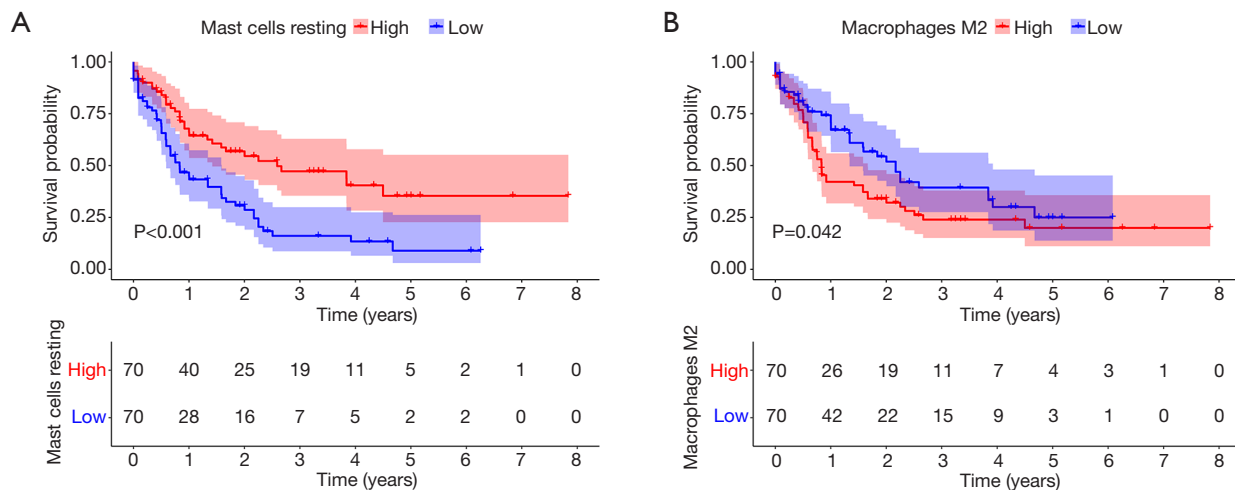


Figure 7 Immune cells that affected the overall survival in AML patients. Kaplan-Meier survival analysis of (A) resting mast cells and (B) M2 macrophages. AML, acute myeloid leukemia.

tumorigenesis, therapy response, drug resistance in various cancer types. FRGs have been shown to be important factors that significantly influence tumor progression in multiple cancer types such as hepatocellular carcinoma, clear cell renal cell carcinoma, and breast cancer (27-29). AML, as the most common hematological malignancy in adult patients, is still an incurable disease and poses a big challenge for public health. A number of studies have shown that ferroptosis-related signatures take part in several important processes in solid cancer, but no study has revealed the underlying mechanism and role of FRGs in AML. We therefore attempted to investigate their expression levels, prognostic role, influence on the TME, and the effect of drug resistance in AML.

The transcriptome data of AML patients was downloaded from TCGA and the transcriptome data of normal samples was obtained from the GTEx database, and FRGs were selected via public articles. We analyzed the expression levels of FRGs between AML and normal samples. A prognostic model based on FRGs was constructed via lasso regression. Among the genes, SLC7A11, GPX4, TFRC, LPCAT3, and DPP4 were further investigated in terms of their expression levels and prognostic role in AML. We performed validation experiments to verify the final selected gene expression levels via immunohistochemistry, PCR, and RNA-seq. Finally, we explored whether there was an association between immune infiltration and drug sensitivity, and finally selected FRGs.

Recently, more and more studies have revealed the

significant role of ferroptosis in cancer. Apart from being a unique form of cell death, ferroptosis has been shown to play important roles in cancer stem cells and the TME (30-32). As the most important regulators in the ferroptosis process, FRGs have been confirmed to play critical roles in the prognosis and resistance of glioma (33,34). In our study, DPP4 was overexpressed, while LPCAT3, TFRC, GPX4, and SLC7A11 were downregulated in AML samples compared to normal samples. Interestingly, several gene expression levels were inconsistent in the public dataset analysis. DPP4, GPX4, LPCAT3, SLC7A11, and TFRC all had higher expression in AML bone marrow samples. TFRC was significantly overexpressed, but DPP4, GPX4, LPCAT3, and SLC7A11 were significantly downregulated in AML samples via PCR analysis. RNA-seq results showed that TFRC was significantly overexpressed while DPP4 was significantly downregulated in AML samples. The prognostic model showed that SLC7A11, GPX4, TFRC, LPCAT3, and DPP4 significantly influenced the prognosis of AML patients. DPP4, LPCAT3, GPX4, and SLC7A11 may act as adverse biomarkers, while controversially, TFRC may act as a protective factor for AML patients. DPP4 acts as an adverse signature for breast, prostate, and pancreatic cancer, and inhibition of DPP4 can improve the prognosis of these patients (35). Zhang *et al.*'s study indicated that overexpression of glutathione peroxidase 4 (GPX4) could enhance cisplatin resistance *in vitro* (36). Guerriero *et al.* revealed that GPX4 was significantly overexpressed in human hepatocellular carcinoma, further indicating that

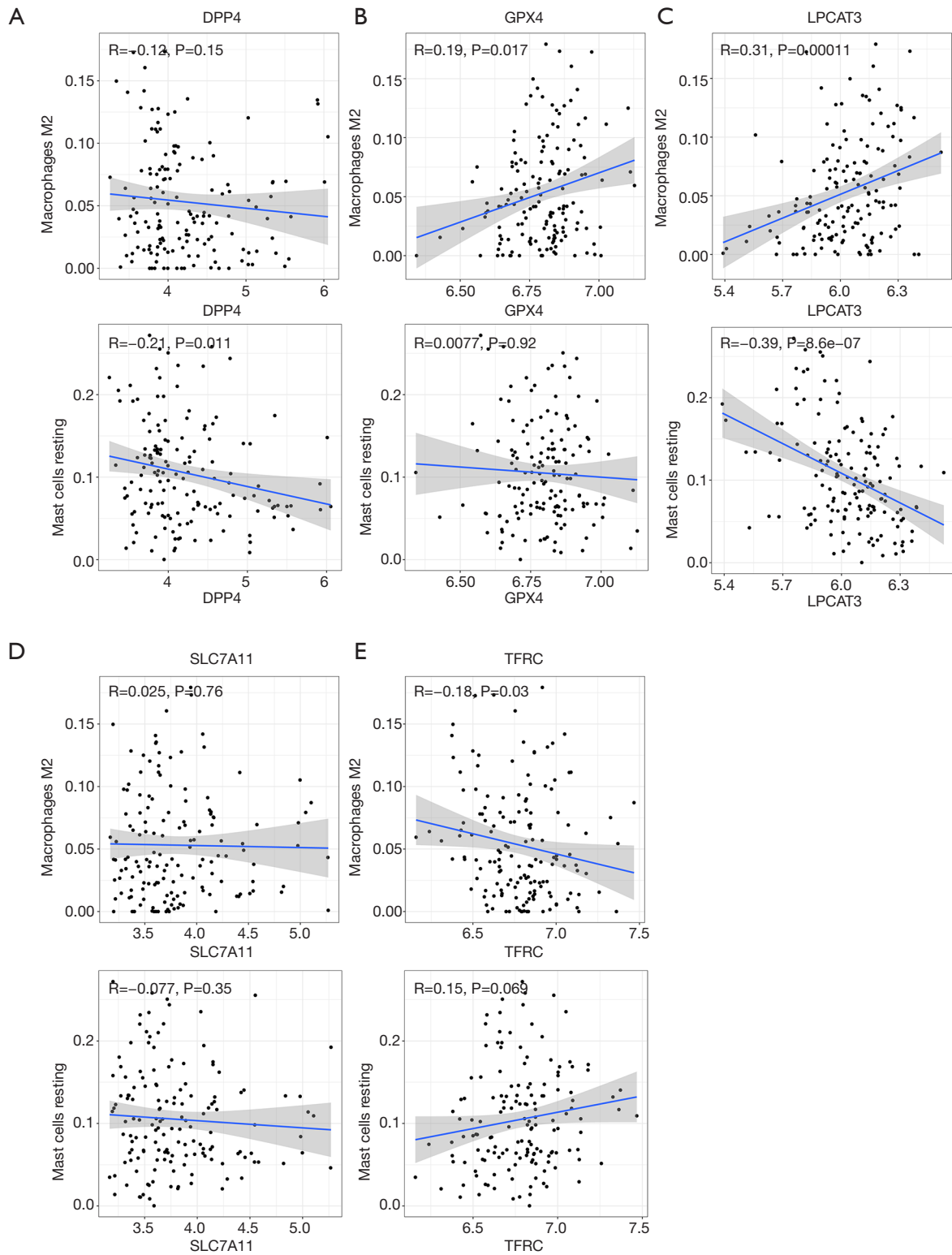


Figure 8 Correlation between the FRG signature biomarker and the abundance of resting mast cells and M2 macrophages. (A) DPP4, (B) GPX4, (C) LPCAT3, (D) SLC7A11, and (E) TFRC. FRG, ferroptosis-related gene.

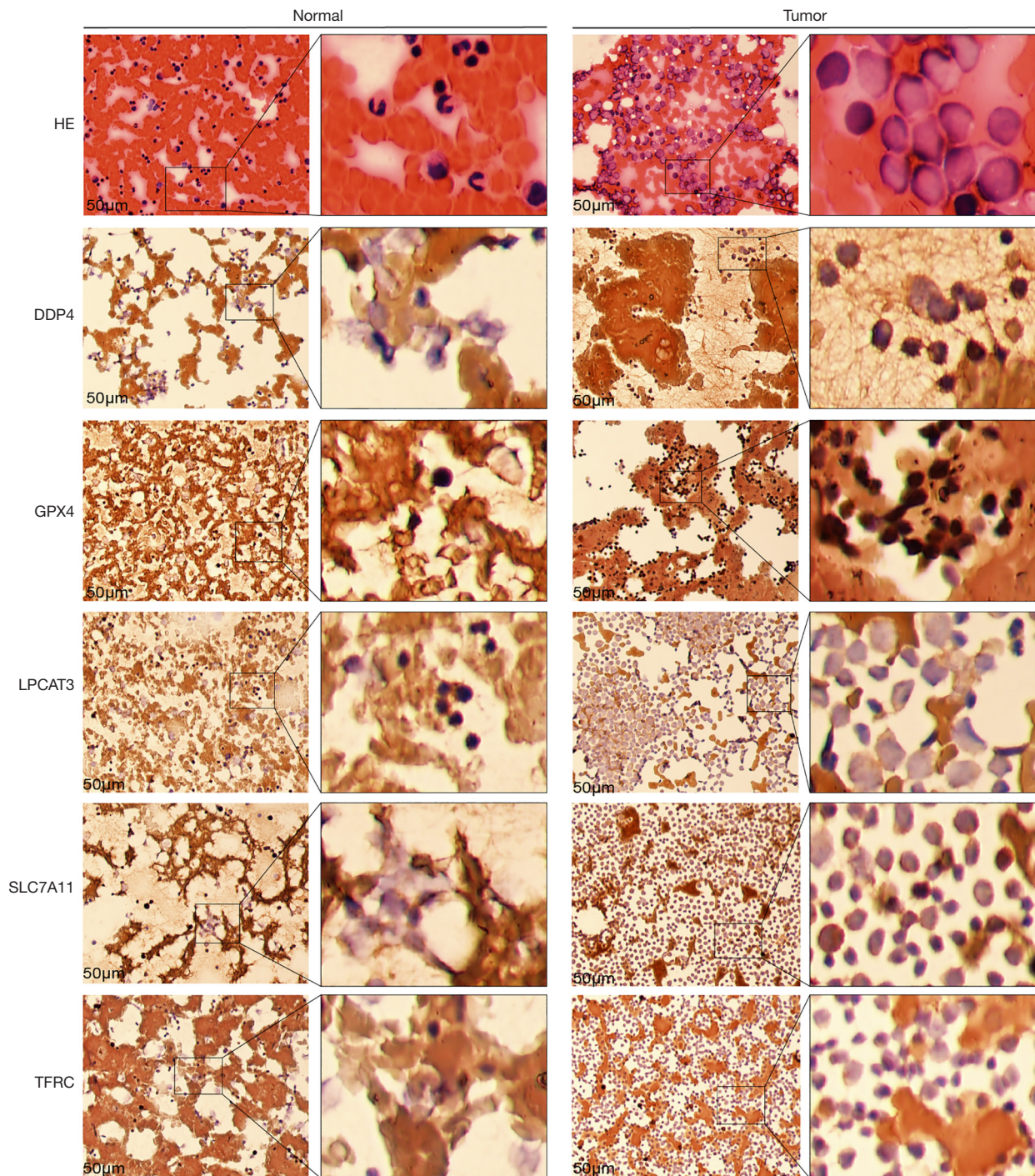


Figure 9 Immunohistochemistry findings of DPP4, GPX4, LPCAT3, SLC7A11, and TFRC expression.

expression levels may be impacted by cancer status (37). Ma *et al.* revealed that SLC7A11 was overexpressed in laryngeal squamous cell carcinoma, and the upregulation of

SLC7A11 promoted tumor progression (38). From these findings, we can conclude that DPP4, LPCAT3, GPX4, and SLC7A11 have essential biological functions in multiple

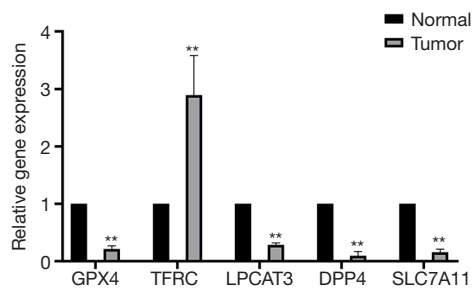


Figure 10 The PCR results of DPP4, GPX4, LPCAT3, SLC7A11, and TFRC expression. **, $P < 0.01$. PCR, polymerase chain reaction.

cancer types, and most of them act as tumor promoters. In regards to AML, only GPX4 has been investigated in terms of its expression and prognostic role. Wei *et al.* showed that GPX4 was significantly downregulated in AML patient samples, and overexpression of GPX4 indicated a better outcome (39). In regards to TFRC, Huang *et al.* revealed that TFRC accelerated the progression of epithelial ovarian cancer via upregulating AXIN2 expression (40). In another study, TFRC also acted as a promoter of liver cancer cells, and inhibition of TFRC could suppress cancer cell growth and survival (41). From these findings, TFRC may be an oncogene for liver cancer and epithelial ovarian cancer, which is inconsistent with its prognostic role in AML patients. There has been no study that has explored the role of TFRC in AML.

Based on the fundamental function of ferroptosis in immune responses, we also performed an analysis of the relationship between final selected FRGs and immune cell infiltration. Based on the validation experiment results, we finally selected DPP4 and TFRC for this analysis. The results showed that TFRC and DPP4 were negatively correlated with resting mast cells but positively correlated with M2 macrophages. The TME is one of the critical regulators of immunotherapy, chemotherapy response, and tumor progression (42-44). Research on the TME in solid tumors has been prosperous, but the underlying mechanisms of the TME in therapy response, prognosis, and tumor progression are still unclear. Based on the complexity of the microenvironment of AML, only a few studies have preliminarily investigated the TME of AML (45-48). Carter

et al. revealed that the TME can significantly influence the drug sensitivity of AML (45). Furthermore, our results showed that resting mast cell infiltration resulted in a better OS, but high infiltration of M2 macrophages resulted in a poor prognosis for AML patients. Lan *et al.* revealed that M2 macrophage-derived exosomes promoted the invasion and migration ability of colon cancer cells (49). M2 macrophages also served as promoters of multiple cancer types such as breast, gastric, and bladder cancer (50,51). The fundamental biological function of resting mast cells in cancer still remains to be elucidated, but several studies have shown that they may have a strong influence on cancer (52-54). Xu *et al.* indicated that M2 macrophages were enriched in AML, and led to poor outcomes (55). The other type of macrophages, M1 macrophages, may serve as protective factors in AML (56). These results also highlight the important role of the TME in AML, but there is still a long way to go.

The ultimate goal of the present study was to find a reasonable novel or complimentary therapy regimen for AML patients. We analyzed the association between DPP4, TFRC, and drug sensitivity in AML patients. The results showed that patients with downregulation of TFRC lead to resistant to ATRA, AZD.2281, CMK, and metformin, and upregulated TFRC induce resistant to bexarotene, bicalutamide, and dasatinib. According to DPP4, patients with high-risk scores were resistant to CMK and cytarabine, and among others, but sensitive to dasatinib. The dysregulated expression of DPP4 can influence the sensitivity to cytarabine, and cytarabine is one of the first-line therapy regimens in AML. Therefore, more reasonable chemotherapy regimens can be selected via this analysis.

Conclusions

In our study, we found that FRGs can serve as diagnostic and prognostic biomarkers for AML patients. FRGs not only have a strong influence on the TME of AML, but also drug resistance. The findings of this study provide useful information for clinicians to select therapy regimens based on FRG expression levels, and pave the way for future fundamental research to understand the underlying mechanisms of ferroptosis in AML.

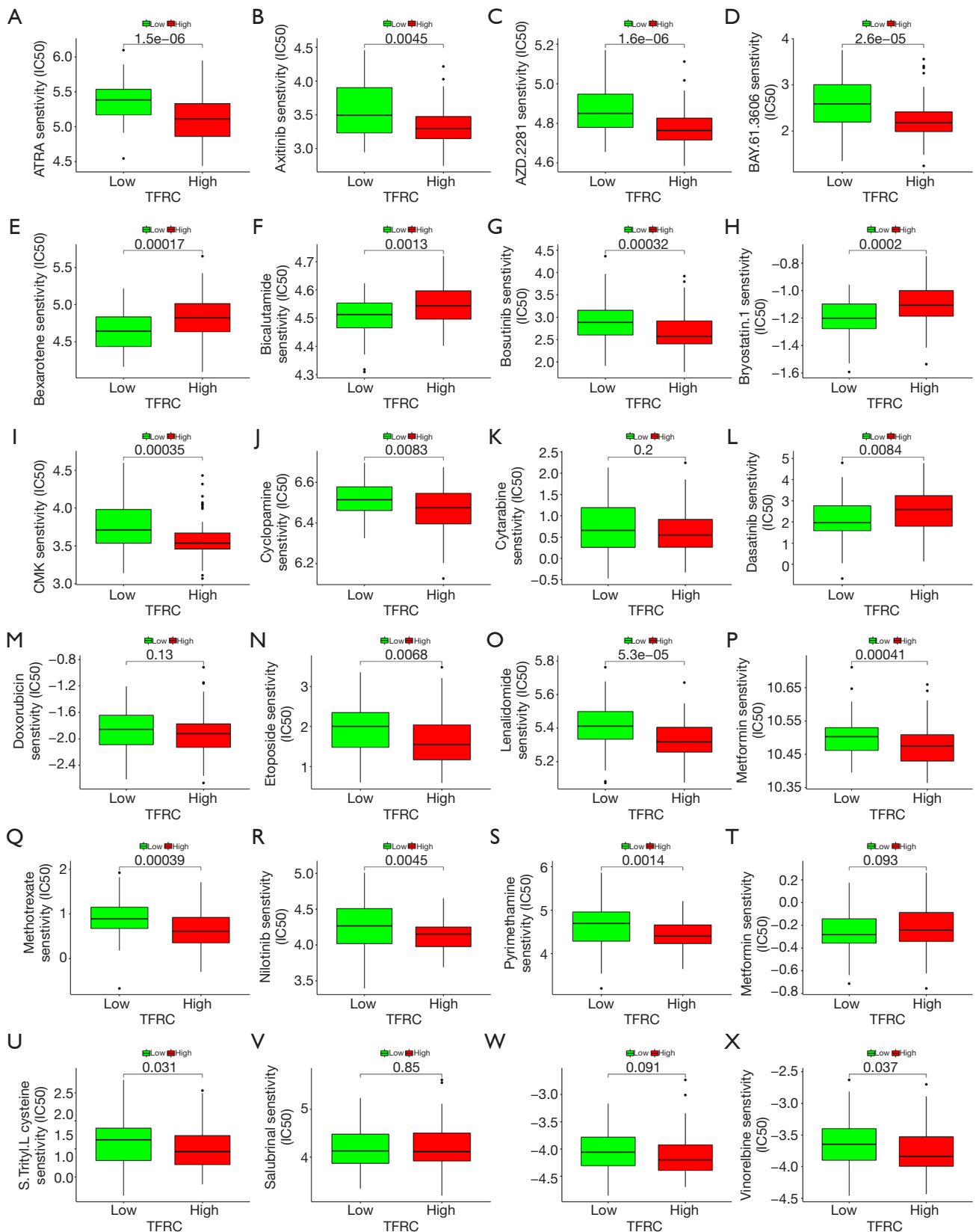


Figure 11 Relationship between risk score and drug sensitivity via the R package pRRophetic (TFRC).

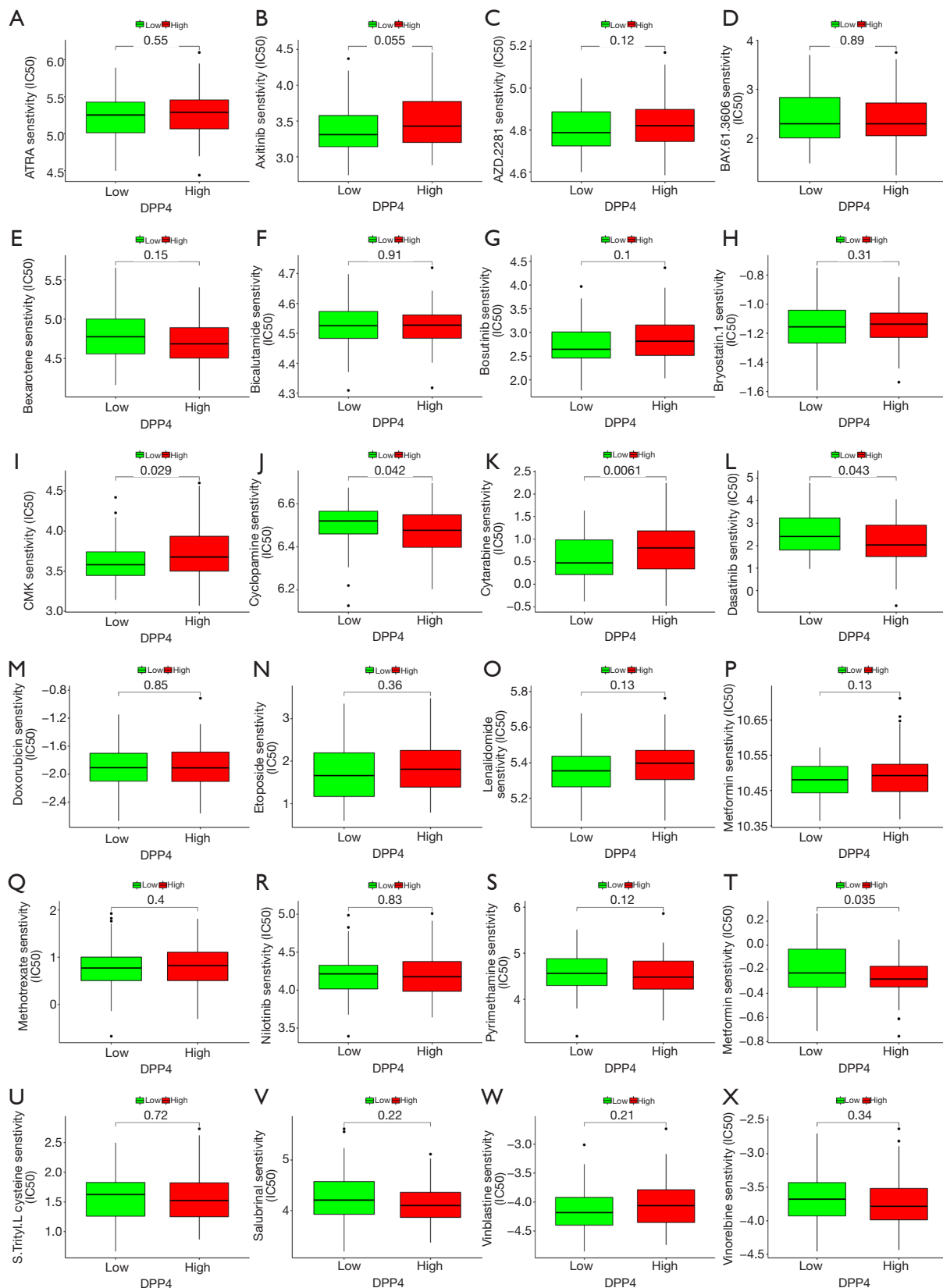


Figure 12 Relationship between risk score and drug sensitivity via the R package pRRophetic (DPP4).

Acknowledgments

Funding: None.

Footnote

Reporting Checklist: The authors have completed the REMARK reporting checklist. Available at <https://dx.doi.org/10.21037/atm-21-3368>

Conflicts of Interest: All authors have completed the ICMJE uniform disclosure form (available at <https://dx.doi.org/10.21037/atm-21-3368>). The authors have no conflicts of interest to declare.

Ethical Statement: The authors are accountable for all aspects of the work in ensuring that questions related to the accuracy or integrity of any part of the work are appropriately investigated and resolved. The study was conducted in accordance with the Declaration of Helsinki (as revised in 2013).

Open Access Statement: This is an Open Access article distributed in accordance with the Creative Commons Attribution-NonCommercial-NoDerivs 4.0 International License (CC BY-NC-ND 4.0), which permits the non-commercial replication and distribution of the article with the strict proviso that no changes or edits are made and the original work is properly cited (including links to both the formal publication through the relevant DOI and the license). See: <https://creativecommons.org/licenses/by-nc-nd/4.0/>.

References

- Callens C, Coulon S, Naudin J, et al. Targeting iron homeostasis induces cellular differentiation and synergizes with differentiating agents in acute myeloid leukemia. *J Exp Med* 2010;207:731-50.
- Roboz GJ. Novel approaches to the treatment of acute myeloid leukemia. *Hematology Am Soc Hematol Educ Program* 2011;2011:43-50.
- Rashidi A, Weisdorf DJ, Bejanyan N. Treatment of relapsed/refractory acute myeloid leukaemia in adults. *Br J Haematol* 2018;181:27-37.
- Kishtagari A, Levine RL, Viny AD. Driver mutations in acute myeloid leukemia. *Curr Opin Hematol* 2020;27:49-57.
- Döhner H, Estey E, Grimwade D, et al. Diagnosis and management of AML in adults: 2017 ELN recommendations from an international expert panel. *Blood* 2017;129:424-47.
- Eguchi M, Minami Y, Kuzume A, et al. Mechanisms Underlying Resistance to FLT3 Inhibitors in Acute Myeloid Leukemia. *Biomedicines* 2020;8:245.
- Weisberg E, Sattler M, Ray A, et al. Drug resistance in mutant FLT3-positive AML. *Oncogene* 2010;29:5120-34.
- Martelli MP, Martino G, Cardinali V, et al. Enasidenib and ivosidenib in AML. *Minerva Med* 2020;111:411-26.
- Antar A, Otrrock ZK, El-Cheikh J, et al. Inhibition of FLT3 in AML: a focus on sorafenib. *Bone Marrow Transplant* 2017;52:344-51.
- Intlekofer AM, Shih AH, Wang B, et al. Acquired resistance to IDH inhibition through trans or cis dimer-interface mutations. *Nature* 2018;559:125-9.
- Kerins MJ, Ooi A. The Roles of NRF2 in Modulating Cellular Iron Homeostasis. *Antioxid Redox Signal* 2018;29:1756-73.
- Dixon SJ, Lemberg KM, Lamprecht MR, et al. Ferroptosis: an iron-dependent form of nonapoptotic cell death. *Cell* 2012;149:1060-72.
- Stockwell BR, Friedmann Angeli JP, Bayir H, et al. Ferroptosis: A Regulated Cell Death Nexus Linking Metabolism, Redox Biology, and Disease. *Cell* 2017;171:273-85.
- Friedmann Angeli JP, Krysko DV, Conrad M. Ferroptosis at the crossroads of cancer-acquired drug resistance and immune evasion. *Nat Rev Cancer* 2019;19:405-14.
- Shi L, Huang Y, Huang X, et al. Analyzing the key gene expression and prognostics values for acute myeloid leukemia. *Transl Cancer Res* 2020;9:7284-98.
- Viswanathan VS, Ryan MJ, Dhruv HD, et al. Dependency of a therapy-resistant state of cancer cells on a lipid peroxidase pathway. *Nature* 2017;547:453-7.
- Liu Y, Xu Z, Jin T, et al. Ferroptosis in Low-Grade Glioma: A New Marker for Diagnosis and Prognosis. *Med Sci Monit* 2020;26:e921947.
- Tang B, Zhu J, Li J, et al. The ferroptosis and iron-metabolism signature robustly predicts clinical diagnosis, prognosis and immune microenvironment for hepatocellular carcinoma. *Cell Commun Signal* 2020;18:174.
- Tang R, Hua J, Xu J, et al. The role of ferroptosis regulators in the prognosis, immune activity and gemcitabine resistance of pancreatic cancer. *Ann Transl Med* 2020;8:1347.
- Zhuo S, Chen Z, Yang Y, et al. Clinical and Biological

- Significances of a Ferroptosis-Related Gene Signature in Glioma. *Front Oncol* 2020;10:590861.
21. Du J, Wang T, Li Y, et al. DHA inhibits proliferation and induces ferroptosis of leukemia cells through autophagy dependent degradation of ferritin. *Free Radic Biol Med* 2019;131:356-69.
 22. Du Y, Bao J, Zhang MJ, et al. Targeting ferroptosis contributes to ATPR-induced AML differentiation via ROS-autophagy-lysosomal pathway. *Gene* 2020;755:144889.
 23. Zhu HY, Huang ZX, Chen GQ, et al. Typhaneoside prevents acute myeloid leukemia (AML) through suppressing proliferation and inducing ferroptosis associated with autophagy. *Biochem Biophys Res Commun* 2019;516:1265-71.
 24. Hassannia B, Vandenabeele P, Vanden Berghe T. Targeting Ferroptosis to Iron Out Cancer. *Cancer Cell* 2019;35:830-49.
 25. Li J, Cao F, Yin HL, et al. Ferroptosis: past, present and future. *Cell Death Dis* 2020;11:88.
 26. Liang C, Zhang X, Yang M, et al. Recent Progress in Ferroptosis Inducers for Cancer Therapy. *Adv Mater* 2019;31:e1904197.
 27. Li Z, Chen L, Chen C, et al. Targeting ferroptosis in breast cancer. *Biomark Res* 2020;8:58.
 28. Liang JY, Wang DS, Lin HC, et al. A Novel Ferroptosis-related Gene Signature for Overall Survival Prediction in Patients with Hepatocellular Carcinoma. *Int J Biol Sci* 2020;16:2430-41.
 29. Wu G, Wang Q, Xu Y, et al. A new survival model based on ferroptosis-related genes for prognostic prediction in clear cell renal cell carcinoma. *Aging (Albany NY)* 2020;12:14933-48.
 30. Bisaro B, Mandili G, Poli A, et al. Proteomic analysis of extracellular vesicles from medullospheres reveals a role for iron in the cancer progression of medulloblastoma. *Mol Cell Ther* 2015;3:8.
 31. Schonberg DL, Miller TE, Wu Q, et al. Preferential Iron Trafficking Characterizes Glioblastoma Stem-like Cells. *Cancer Cell* 2015;28:441-55.
 32. Zhu T, Shi L, Yu C, et al. Ferroptosis Promotes Photodynamic Therapy: Supramolecular Photosensitizer-Inducer Nanodrug for Enhanced Cancer Treatment. *Theranostics* 2019;9:3293-307.
 33. Liu HJ, Hu HM, Li GZ, et al. Ferroptosis-Related Gene Signature Predicts Glioma Cell Death and Glioma Patient Progression. *Front Cell Dev Biol* 2020;8:538.
 34. Wan RJ, Peng W, Xia QX, et al. Ferroptosis-related gene signature predicts prognosis and immunotherapy in glioma. *CNS Neurosci Ther* 2021;27:973-86.
 35. Shah C, Hong YR, Bishnoi R, et al. Impact of DPP4 Inhibitors in Survival of Patients With Prostate, Pancreas, and Breast Cancer. *Front Oncol* 2020;10:405.
 36. Zhang X, Sui S, Wang L, et al. Inhibition of tumor propellant glutathione peroxidase 4 induces ferroptosis in cancer cells and enhances anticancer effect of cisplatin. *J Cell Physiol* 2020;235:3425-37.
 37. Guerriero E, Capone F, Accardo M, et al. GPX4 and GPX7 over-expression in human hepatocellular carcinoma tissues. *Eur J Histochem* 2015;59:2540.
 38. Ma Z, Zhang H, Lian M, et al. SLC7A11, a component of cysteine/glutamate transporter, is a novel biomarker for the diagnosis and prognosis in laryngeal squamous cell carcinoma. *Oncol Rep* 2017;38:3019-29.
 39. Wei J, Xie Q, Liu X, et al. Identification the prognostic value of glutathione peroxidases expression levels in acute myeloid leukemia. *Ann Transl Med* 2020;8:678.
 40. Huang Y, Huang J, Huang Y, et al. TFRC promotes epithelial ovarian cancer cell proliferation and metastasis via up-regulation of AXIN2 expression. *Am J Cancer Res* 2020;10:131-47.
 41. Muhammad JS, Bajbouj K, Shafarin J, et al. Estrogen-induced epigenetic silencing of FTH1 and TFRC genes reduces liver cancer cell growth and survival. *Epigenetics* 2020;15:1302-18.
 42. Farhood B, Najafi M, Mortezaee K. CD8(+) cytotoxic T lymphocytes in cancer immunotherapy: A review. *J Cell Physiol* 2019;234:8509-21.
 43. Hinshaw DC, Shevde LA. The Tumor Microenvironment Innately Modulates Cancer Progression. *Cancer Res* 2019;79:4557-66.
 44. Junttila MR, de Sauvage FJ. Influence of tumour micro-environment heterogeneity on therapeutic response. *Nature* 2013;501:346-54.
 45. Carter BZ, Mak PY, Wang X, et al. An ARC-Regulated IL1beta/Cox-2/PGE2/beta-Catenin/ARC Circuit Controls Leukemia-Microenvironment Interactions and Confers Drug Resistance in AML. *Cancer Res* 2019;79:1165-77.
 46. Nahas MR, Stroopinsky D, Rosenblatt J, et al. Hypomethylating agent alters the immune microenvironment in acute myeloid leukaemia (AML) and enhances the immunogenicity of a dendritic cell/AML vaccine. *Br J Haematol* 2019;185:679-90.
 47. Shafat MS, Gnaneswaran B, Bowles KM, et al. The bone marrow microenvironment - Home of the leukemic blasts.

- Blood Rev 2017;31:277-86.
48. van Galen P, Hovestadt V, Wadsworth Ii MH, et al. Single-Cell RNA-Seq Reveals AML Hierarchies Relevant to Disease Progression and Immunity. *Cell* 2019;176:1265-81.e24.
 49. Lan J, Sun L, Xu F, et al. M2 Macrophage-Derived Exosomes Promote Cell Migration and Invasion in Colon Cancer. *Cancer Res* 2019;79:146-58.
 50. Chen Y, Zhang S, Wang Q, et al. Tumor-recruited M2 macrophages promote gastric and breast cancer metastasis via M2 macrophage-secreted CHI3L1 protein. *J Hematol Oncol* 2017;10:36.
 51. Martínez VG, Rubio C, Martínez-Fernandez M, et al. BMP4 Induces M2 Macrophage Polarization and Favors Tumor Progression in Bladder Cancer. *Clin Cancer Res* 2017;23:7388-99.
 52. Li J, Li X, Zhang C, et al. A signature of tumor immune microenvironment genes associated with the prognosis of nonsmall cell lung cancer. *Oncol Rep* 2020;43:795-806.
 53. Pan Q, Wang L, Chai S, et al. The immune infiltration in clear cell Renal Cell Carcinoma and their clinical implications: A study based on TCGA and GEO databases. *J Cancer* 2020;11:3207-15.
 54. Tang X, Shu Z, Zhang W, et al. Clinical significance of the immune cell landscape in hepatocellular carcinoma patients with different degrees of fibrosis. *Ann Transl Med* 2019;7:528.
 55. Xu ZJ, Gu Y, Wang CZ, et al. The M2 macrophage marker CD206: a novel prognostic indicator for acute myeloid leukemia. *Oncoimmunology* 2020;9:1683347.
 56. Yang X, Feng W, Wang R, et al. Repolarizing heterogeneous leukemia-associated macrophages with more M1 characteristics eliminates their pro-leukemic effects. *Oncoimmunology* 2018;7:e1412910.

(English Language Editor: C. Betlazar-Maseh)

Cite this article as: Wei J, Nai GY, Dai Y, Huang XJ, Xiong MY, Yao XY, Huang ZN, Li SN, Zhou WJ, Huang Y, Cheng P, Deng DH. Dipetidyl peptidase-4 and transferrin receptor serve as prognostic biomarkers for acute myeloid leukemia. *Ann Transl Med* 2021;9(17):1381. doi: 10.21037/atm-21-3368